



PII:S0031-3203(96)00065-9

THRESHOLD SELECTION USING RENYI'S ENTROPY

PRASANNA SAHOO*, CARRYE WILKINS and JERRY YEAGER

Department of Mathematics, University of Louisville, Louisville, KY 40292, U.S.A.

(Received 22 August 1995; in revised form 3 April 1996; received for publication 10 May 1996)

Abstract—Image segmentation is an important and fundamental task in many digital image processing systems. Image segmentation by thresholding is the simplest technique and involves the basic assumption that objects and background in the digital image have distinct gray-level distributions. In this paper, we present a general technique for thresholding of digital images based on Renyi's entropy. Our method includes two of the previously proposed well known global thresholding methods. The effectiveness of the proposed method is demonstrated by using examples from the real-world and synthetic images.

Renyi entropy	Shannon entropy	Image thresholding
Maximum entropy sum method	Entropic correlation method	

1. INTRODUCTION

One of the most frequently used methods in image processing is thresholding. It distinguishes objects from the background in images. Thus it is used as a popular tool in a variety of image processing applications such as text enhancement, biomedical image analysis, automatic target recognition,⁽¹⁾ and locating addresses on envelopes.⁽²⁾ For a survey of thresholding methods, the interested reader should refer to papers by Sahoo *et al.*⁽³⁾ and Weszka.⁽⁴⁾

The threshold selection techniques can be divided into two groups such as bilevel and multilevel. In bilevel thresholding, one threshold value is used for segmenting an image into a background and an object. Bilevel thresholding is used if an image has an object distinct from the background. In an image, if the object is distinct from the background, then the histogram of the gray level will be bimodal, and a threshold can be chosen to coincide with the valley of the gray-level histogram. Each pixel that has a gray value above the threshold will be assigned to the background (object) and each pixel with gray value below or equal to the threshold will be assigned to the object (background). Although bilevel thresholding methods are simple, there are some instances where images have gray-level histograms that are not bimodal and many known methods do not produce effective threshold values.

Multilevel thresholding is used when an image has several objects that are distinct from the background. The presence of several distinct objects makes the histogram multimodal. The threshold is found by locating the valleys that separate the objects. Thus the multilevel method is an extension of the bilevel method. If the gray-level histogram is neither bimodal nor multimodal, then it may be unimodal. A unimodal histogram has only one peak and thus there is no valley

between the two groups. In such cases where there is no valley, other techniques besides valley seeking methods must be used. These techniques use a criterion function to determine the optimal threshold.

In this paper, we propose an automatic global thresholding method using Renyi's entropy. The proposed method extends two well known global thresholding methods, one due to Kapur *et al.*⁽⁵⁾ and the other due to Chang *et al.*⁽⁶⁾ This paper is organized as follows: In Section 2, we present a brief survey of entropic thresholding methods that have been reported recently in the literature. Section 3 describes the mathematical setting of the threshold selection. In this section, the maximum entropy sum method⁽⁵⁾ and the entropic correlation method⁽⁶⁾ are outlined for later use. In Section 4, the new thresholding method is described. Section 5 reports the effectiveness of our thresholding method when applied to some real-world and synthetic images. In Section 6, we present some concluding remarks about our method.

2. REVIEW OF RECENT INFORMATION THEORETIC GLOBAL METHODS

Over the last two decades, many threshold selection methods have been proposed.^(1–47) For a survey of many of these methods see references (3) and (4) and references therein. Information theoretic methods for image thresholding use the image histogram and an objective function derived using information theory to determine the optimal threshold.

The first entropy based method was proposed by Pun.⁽³⁵⁾ Knowing the *a priori* entropy of the gray-level histogram, Pun [see reference (5)] proposed an algorithm to determine the optimal threshold by maximizing the upper bound of the *a posteriori* entropy. This method has some theoretical problems which were addressed in reference (5). Correcting the mathematical error in

* Author to whom correspondence should be addressed.

reference (5), Kapur *et al.* proposed a new entropic method for image thresholding. Like the method of Pun, this method obtained the optimal threshold by maximizing the *a priori* entropies of the object and the background classes. In reference (5), the authors raised the following concern in the conclusion of their paper: "What happens if two different pictures have the same gray-level histogram and thus the same threshold? Will it be suitable for both?" They also suggested that a second-order statistic or some local property with the entropic concept of thresholding might give a better insight into these problems. In reference (7), Abutaleb extended the method of Kapur, Sahoo and Wong using two-dimensional entropies. The two-dimensional entropies were obtained from the two-dimensional histogram which was determined by using the gray value of the pixel and the local average gray value of the pixel. This extension due to Abutaleb was also investigated by Brink.⁽¹⁰⁾ Pal and Pal⁽³²⁾ have also considered thresholding using some second-order statistics.

Johannsen and Bille⁽²¹⁾ proposed a method using the entropy of the gray-level histogram. This method divides the set of gray levels into two parts so as to minimize the interdependence (in information theoretic sense) between them. Wong and Sahoo⁽⁴⁵⁾ proposed a thresholding method based on the maximum entropy principle. The optimal threshold value is determined by maximizing the *a posteriori* entropy subject to certain inequality constraints which are derived by means of special measures characterizing uniformity and the shape of the regions in the image. For this purpose, the authors use both the gray-level distribution and the spatial information of an image. This method was discovered while investigating the questions Kapur, Sahoo and Wong had raised in reference (5). Recently, Li and Lee⁽²⁶⁾ have proposed an information theoretic method based on Kullback's minimum cross-entropy principle. The cross entropy is formulated in a pixel-to-pixel basis between the background and foreground. The optimal threshold is obtained by minimizing this cross entropy. This method can be considered as a method which uses the spatial information along with the gray-level distribution.

3. GRAY-LEVEL HISTOGRAM BASED THRESHOLDING

Global threshold selection methods usually use the gray-level histogram of the image. The optimal threshold is determined by optimizing some criterion function obtained from the gray-level distribution of the image.

Let $f(m, n)$ be the gray value of the pixel located at the point (m, n) . In a digital image $\{f(m, n) \mid m \in \{1, 2, \dots, M\}, n \in \{1, 2, \dots, N\}\}$ of size $M \times N$, let the histogram be $h(x)$ for $x \in \{0, 1, 2, \dots, 255\}$. For the sake of convenience, we denote the set of all gray levels $\{0, 1, 2, \dots, 255\}$ as G .

Let t be a threshold value and $B = \{b_0, b_1\}$ be a pair of binary gray levels with $b_0, b_1 \in G$. The result of thresholding an image function $f(m, n)$ at gray level t is

a binary function $f_t(m, n)$ such that

$$f_t(m, n) = \begin{cases} b_0 & \text{if } f(m, n) \leq t, \\ b_1 & \text{if } f(m, n) > t. \end{cases}$$

In general, a thresholding method determines the value t^* of t based on a certain criterion function. If t^* is determined solely from the gray level of each pixel, the thresholding method is point dependent.⁽³⁸⁾

Over the years, many researchers in image processing have treated $\{f(m, n) \mid m \in \{1, 2, \dots, M\}, n \in \{1, 2, \dots, N\}\}$ as a sequence of independent and identically distributed random variables with the density function $h(x)$. The density function $h(x)$ can be obtained from

$$h(x) = \text{Prob}(f(m, n) = x),$$

where $x \in G$. Given an image, there are several methods to estimate this density function. One of the most frequently used methods is the *method of relative frequency*. In this method, the density function (or the normalized histogram) $h(x)$ is approximated by using the formula

$$\begin{aligned} \widehat{h(x)} &= \frac{\text{number of elements in the event } (f(m, n) = x)}{\text{number of elements in the sample space}} \\ &= \frac{\text{number of pixels with the gray value } x}{\text{number of pixels in the image}}, \end{aligned}$$

where $\widehat{h(x)}$ denotes the estimate of $h(x)$.

3.1. The maximum entropy sum method

The maximum entropy sum method proposed by Kapur *et al.*⁽⁵⁾ is based on the maximization of the information measure between two classes (object and background). Consider a discrete image with $N \times M$ pixels defining the object and background. Let $p_i = \hat{h}(i) = n_i/NM$ be an estimate of the probability gray-level value, where n_i represents the number of pixels with gray value i . The *a priori* entropy of the entire image is given by

$$H_T = - \sum_{i=0}^{255} p_i \ln p_i.$$

If we assume two classes of pixels, Λ_1 and Λ_2 (in our case Λ_1 denotes the class of black pixels and Λ_2 denotes the class of white pixels), in the image, the *a priori* entropies are defined as

$$\left. \begin{aligned} H_{\Lambda_1}(t) &= - \sum_{i=0}^t \frac{p_i}{p(\Lambda_1)} \ln \frac{p_i}{p(\Lambda_1)}, \\ H_{\Lambda_2}(t) &= - \sum_{i=t+1}^{255} \frac{p_i}{p(\Lambda_2)} \ln \frac{p_i}{p(\Lambda_2)}, \end{aligned} \right\}$$

where

$$p(\Lambda_1) = \sum_{i=0}^t p_i, p(\Lambda_2) = \sum_{i=t+1}^{255} p_i \quad \text{and } p(\Lambda_1) + p(\Lambda_2) = 1.$$

The information between the two classes, $I(\Lambda_1, \Lambda_2)$, is defined as

$$I(\Lambda_1, \Lambda_2) = H_{\Lambda_1}(t) + H_{\Lambda_2}(t)$$

and can be rewritten as a function, $\phi(t)$, of the threshold t . The above equation can be simplified as

$$\phi(T) = \ln[p(\Lambda_1)p(\Lambda_2)] + \frac{H(t)}{p(\Lambda_1)} + \frac{H_T - H(t)}{1 - p(\Lambda_1)},$$

where $H(t)$ is defined as

$$H(t) = - \sum_{i=0}^t p_i \ln p_i.$$

The method due to Kapur *et al.* chooses the threshold to be the value, t^* , at which the function $\phi(t)$ is maximum. Since some p_i will be very small or even zero, one must be careful when evaluating $p_i \ln p_i$. The optimal threshold value found will lose its usefulness due to potentially large computational errors that result when calculating the logarithms of very small numbers.

3.2. The entropic correlation method

The entropic correlation method proposed by Chang *et al.*⁽⁶⁾ maximizes the entropic correlation between the object and background classes. The authors define the correlation¹ of X as

$$C_X(t) = -\ln \sum_{i \geq 0} p_i^2,$$

where X is a discrete random variable with finite or countably infinite range $B = x_0, x_1, x_2, \dots$ and p_i is the probability of $X = x_i$. Based on this definition, the correlation provided by the classes Λ_1 and Λ_2 can be calculated. The correlations associated with the distributions Λ_1 and Λ_2 are defined [see reference (6)] by

$$C_{\Lambda_1}(t) = -\ln \sum_{i=0}^t \left(\frac{p_i}{p(\Lambda_1)} \right)^2$$

and

$$C_{\Lambda_2}(t) = -\ln \sum_{i=t+1}^{255} \left(\frac{p_i}{1 - p(\Lambda_1)} \right)^2,$$

respectively. The total available correlation, which will be denoted by TC, provided by Λ_1 and Λ_2 is

$$\begin{aligned} TC(t) &= C_{\Lambda_1}(t) + C_{\Lambda_2}(t) \\ &= -\ln \sum_{i=0}^t \left(\frac{p_i}{p(\Lambda_1)} \right)^2 - \ln \sum_{i=t+1}^{255} \left(\frac{p_i}{1 - p(\Lambda_1)} \right)^2 \\ &= -\ln \left(\frac{G_{\Lambda_1}(t)G_{\Lambda_2}(t)}{p(\Lambda_1)^2(1 - p(\Lambda_1))^2} \right) \\ &= -\ln(G_{\Lambda_1}(t)G_{\Lambda_2}(t)) + 2 \ln(p(\Lambda_1)(1 - p(\Lambda_1))), \end{aligned}$$

where

$$G_{\Lambda_1}(t) = \sum_{i=0}^t p_i^2$$

and

$$G_{\Lambda_2}(t) = \sum_{i=t+1}^{255} p_i^2.$$

In the entropic correlation method, Chang *et al.*⁽⁶⁾ used

$$\psi(t) = -\ln(G_{\Lambda_1}(t)G_{\Lambda_2}(t)) + 2 \ln(p(\Lambda_1)(1 - p(\Lambda_1)))$$

as a criterion function to obtain the optimal threshold for an image.

4. THRESHOLDING WITH RENYI'S ENTROPY

Similar to the maximum entropy sum method of Kapur *et al.*⁽⁵⁾ and the entropic correlation method of Chang *et al.*⁽⁶⁾, we proposed a new thresholding technique using Renyi's entropy. Our entropic thresholding method uses two probability distributions (object and background) derived from the original gray-level distribution of an image and includes the maximum entropy sum method and the entropic correlation method.

Let $p_0, p_1, p_2, \dots, p_{255}$ be the probability distribution of gray levels. From this distribution, two probability distributions, one for the object class Λ_1 and the other for the background class Λ_2 , are derived. The probability distributions of the object and background classes, Λ_1 and Λ_2 , are given by

$$\Lambda_1 : \frac{p_0}{p(\Lambda_1)}, \frac{p_1}{p(\Lambda_1)}, \dots, \frac{p_t}{p(\Lambda_1)}$$

and

$$\Lambda_2 : \frac{p_{t+1}}{p(\Lambda_2)}, \frac{p_{t+2}}{p(\Lambda_2)}, \dots, \frac{p_{255}}{p(\Lambda_2)},$$

where

$$p(\Lambda_1) = \sum_{i=0}^t p_i, p(\Lambda_2) = \sum_{i=t+1}^{255} p_i \quad \text{and} \quad p(\Lambda_1) + p(\Lambda_2) = 1.$$

The *a priori* Renyi's entropy of order α of an image is defined as [see reference (48)]

$$H_T^\alpha = \frac{1}{1 - \alpha} \ln \sum_{k=0}^{255} (p_k)^\alpha,$$

where $\alpha (\neq 1)$ is a positive real parameter. The Renyi's entropy H_T^α is a one parameter generalization of the Shannon entropy H_T since $\lim_{\alpha \rightarrow 1} H_T^\alpha = H_T$. The Renyi's entropies associated with object and background distributions are given by

$$H_{\Lambda_1}^\alpha(t) = \frac{1}{1 - \alpha} \ln \sum_{i=0}^t \left(\frac{p_i}{p(\Lambda_1)} \right)^\alpha$$

and

$$H_{\Lambda_2}^\alpha(t) = \frac{1}{1 - \alpha} \ln \sum_{i=t+1}^{255} \left(\frac{p_i}{p(\Lambda_2)} \right)^\alpha,$$

respectively. Let $t^*(\alpha)$ be the gray level which maximizes $H_{\Lambda_1}^\alpha(t) + H_{\Lambda_2}^\alpha(t)$, that is

$$t^*(\alpha) = \text{Arg max}_{t \in G} \{ H_{\Lambda_1}^\alpha(t) + H_{\Lambda_2}^\alpha(t) \}.$$

¹The use of the term "correlation" seems to be confusing as it is used with two distributions instead of one.

It is evident that $t^*(\alpha)$ is a function of α . From computer simulations we observed that

$$t^*(\alpha) = \begin{cases} t_1^* & \text{if } 0 < \alpha < 1, \\ t_2^* & \text{if } \alpha \rightarrow 1, \\ t_3^* & \text{if } 1 < \alpha < \infty, \end{cases}$$

where t_1^* , t_2^* and t_3^* are distinct gray values. When α approaches 1, the gray value t_2^* is the same as the optimal threshold value found using the maximum entropy sum method and when $\alpha > 1$, the gray value t_3^* is the same as the optimal threshold value obtained by using the entropic correlation method.

The optimal threshold value, t_c^* , of the proposed method is computed using these three distinct gray values t_1^* , t_2^* and t_3^* by the following formula:

$$t_c^* = t_{[1]} \left[p(t_{[1]}) + \frac{1}{4} \omega \beta_1 \right] + \frac{1}{4} t_{[2]} \omega \beta_2 + t_{[3]} \left[1 - p(t_{[3]}) + \frac{1}{4} \omega \beta_3 \right],$$

where $t_{[1]}$, $t_{[2]}$ and $t_{[3]}$ are the order statistics of the gray values t_1^* , t_2^* , t_3^* , $p(t) = \sum_{i=1}^t p_i$, $\omega = p(t_{[3]}) - p(t_{[1]})$, and

$$(\beta_1, \beta_2, \beta_3) = \begin{cases} (1, 2, 1) & \text{if } |t_{[1]} - t_{[2]}| \leq 5 \text{ and } |t_{[2]} - t_{[3]}| \leq 5, \\ (1, 2, 1) & \text{if } |t_{[1]} - t_{[2]}| > 5 \text{ and } |t_{[2]} - t_{[3]}| > 5, \\ (0, 1, 3) & \text{if } |t_{[1]} - t_{[2]}| \leq 5 \text{ and } |t_{[2]} - t_{[3]}| > 5, \\ (3, 1, 0) & \text{if } |t_{[1]} - t_{[2]}| > 5 \text{ and } |t_{[2]} - t_{[3]}| \leq 5. \end{cases}$$

The optimal threshold value t_c^* can be viewed as an image dependent weighted average of t_1^* , t_2^* , t_3^* , and thus

$$\min\{t_1^*, t_2^*, t_3^*\} \leq t_c^* \leq \max\{t_1^*, t_2^*, t_3^*\},$$

that is, $t_{[1]} \leq t_c^* \leq t_{[3]}$. This indicates that even though the maximum entropy sum method or the entropic correlation method fails to provide a good threshold value for an image, the proposed method may provide a good threshold value.

Although the gray values $t_{[1]}$, $t_{[2]}$ and $t_{[3]}$ are distinct, they may or may not be significantly different from each other. If two such values do not differ by five units, then we consider them to be nearly the same and adjust $\beta_1, \beta_2, \beta_3$ accordingly. This convention yields four situations, namely

$$\begin{aligned} &|t_{[1]} - t_{[2]}| \leq 5 \quad \text{and} \quad |t_{[2]} - t_{[3]}| \leq 5, \\ &|t_{[1]} - t_{[2]}| > 5 \quad \text{and} \quad |t_{[2]} - t_{[3]}| > 5, \\ &|t_{[1]} - t_{[2]}| \leq 5 \quad \text{and} \quad |t_{[2]} - t_{[3]}| > 5, \\ &|t_{[1]} - t_{[2]}| > 5 \quad \text{and} \quad |t_{[2]} - t_{[3]}| \leq 5. \end{aligned}$$

These situations are taken into account while assigning values to $\beta_1, \beta_2, \beta_3$.

5. ANALYSIS OF TEST RESULTS

In this section, we discuss the experimental results obtained while using the proposed method. This discussion includes the choice of the optimal threshold

and the presentation of the optimal threshold values of some real-world and synthetic images. These images are *Building*, *Cameraman*, *Girl*, *Holly*, *Landsat Scene*, *Lena*, *Greeting Card*, *Rat Lung*, and *UofL Campus*. The optimal threshold was computed by the proposed method for these nine images. Further, we computed threshold values for these images using the maximum entropy sum method and the entropic correlation method to compare to the threshold values found using our proposed method. We also calculated the ideal threshold value for each image by visually inspecting the affect of a variety of different threshold values on that image and choosing the one which yielded the best aesthetic results. This ideal threshold value² found is denoted by t^* . Table 1 lists the ideal and optimal threshold values that are found for these images.

The original digitized images together with their histograms, the thresholded images obtained by using the optimal threshold value t_c^* and the ideal threshold value t^* are displayed side by side in Figs 1–27. Images obtained by using the optimal threshold values t_2^* and t_3^* are displayed in Figs 28–41. Our analysis is based on how much information is lost due to thresholding. Between two thresholded images of the same original image, we prefer the one which lost the least amount of information.

All images when thresholded at their optimal threshold values t_2^* , t_3^* , t_c^* and the ideal threshold value t^* , yielded comparable images except for the *Lena*, *Greeting Card*, and *UofL Campus* images.³ These images were totally lost when thresholded using the entropic correlation method. The maximum entropy sum method and the new method generated acceptable images (see Figs 37, 38, 41, 17, 20 and 26, respectively). For the *Landsat Scene* image, the optimal threshold value found is 176 when the entropic correlation method was used. When the image was thresholded at 176, the thresholded image lost many important features of the original image (see Fig. 36). Thus, the entropic correlation method did not produce a

Table 1. The ideal and optimal threshold values

Test images	t_1^*	t_2^*	t_3^*	t_{c*}	t_*
Buildings	126	99	145	135	199
Cameraman	81	41	18	36	75
Girl	106	114	139	122	157
Holly	122	120	168	150	132
Landsat Scene	81	176	176	112	128
Lena	38	132	37	119	128
Greeting Card	195	119	194	131	112
Rat Lung	119	134	154	148	153
UofL Campus	137	171	244	155	177

²The ideal threshold value was subjective to authors' perception of what a good thresholded image should look like.

³In computation of t_2^* , we have used H_T instead of H_T^α since $\lim_{\alpha \rightarrow 1} H_T^\alpha = H_T$.



Fig. 1. Original digitized image of building and its histogram.

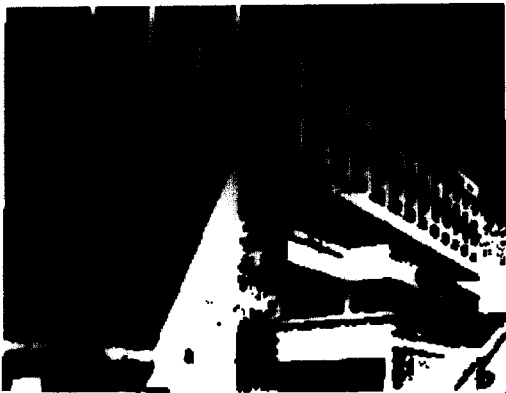


Fig. 2. Thresholded at $t_c^* = 135$.



Fig. 3. Thresholded at $t^* = 199$.



Fig. 4. Original digitized image of a cameraman and its histogram.



Fig. 5. Thresholded at $t_c^* = 36$.



Fig. 6. Thresholded at $t^* = 75$.

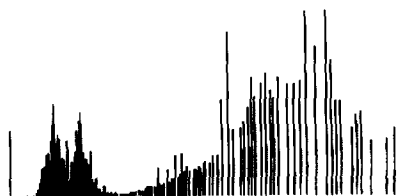


Fig. 7. Original digitized image of a girl and its histogram.



Fig. 8. Thresholded at $t_c^* = 122$.



Fig. 9. Thresholded at $t^* = 157$.

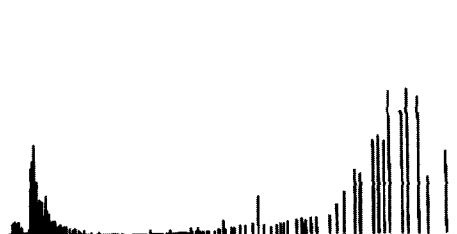


Fig. 10. Original digitized image of Holly and its histogram.



Fig. 11. Thresholded at $t_c^* = 150$.



Fig. 12. Thresholded at $t^* = 132$.

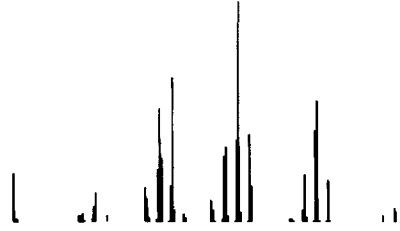
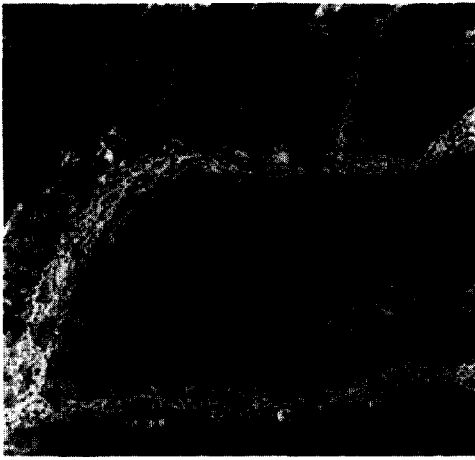


Fig. 13 Fig. 13. Original digitized image of Landast Scene and its histogram.



Fig. 14. Thresholded at $t_c^* = 112$.



Fig. 15. Thresholded at $t^* = 128$.

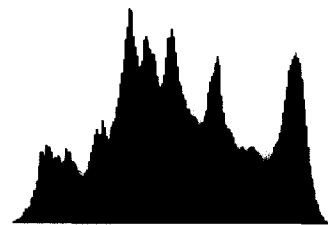


Fig. 16. Original digitized image of Lena and its histogram.

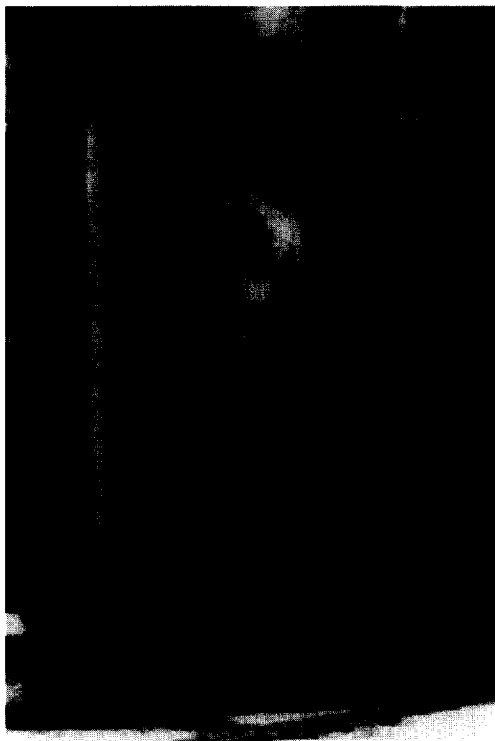
Fig. 17. Thresholded at $t_c^* = 119$.Fig. 18. Thresholded at $t^* = 128$.

Fig. 19. Original digitized image of Greeting Card and its histogram.

good threshold value for the *Landsat Scene* image. Similarly, the entropic correlation method did not produce a reasonable threshold value for the *Camera-man* image which is displayed in Fig. 31. The maximum entropy sum method also did not produce a good threshold value for the *Landsat Scene* image. In fact, we found this threshold value to be the same as the one

obtained by the entropic correlation method. Similarly, the maximum entropy sum method did not produce a good threshold value for the *Building* image (Fig. 28). The optimal threshold value obtained by using the maximum entropy sum method, the entropic correlation method, and the new method for the images of *Girl*, *Holly*, and *Rat Lung* all yielded acceptable images.

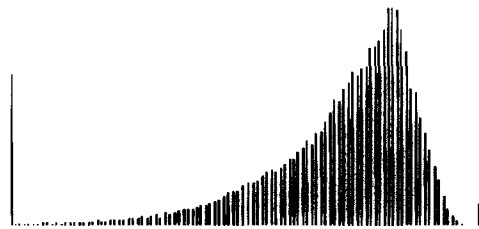
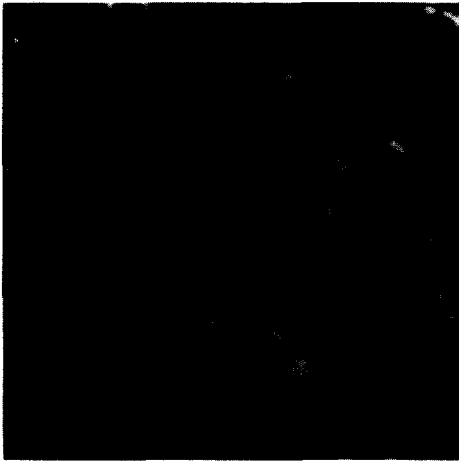
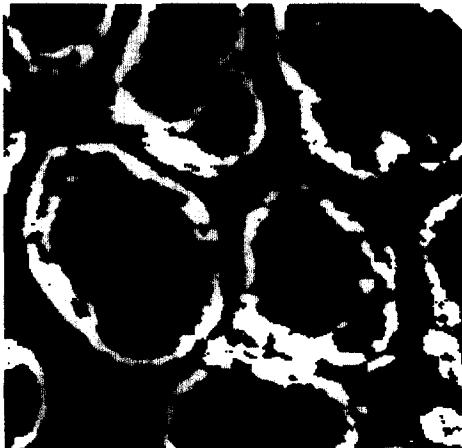
Fig. 20. Thresholded at $t_c^* = 131$.Fig. 21. Thresholded at $t^* = 112$.

Fig. 22. Original digitized image of Rat Lung and its histogram.

Fig. 23. Thresholded at $t_c^* = 148$.Fig. 24. Thresholded at $t^* = 153$.

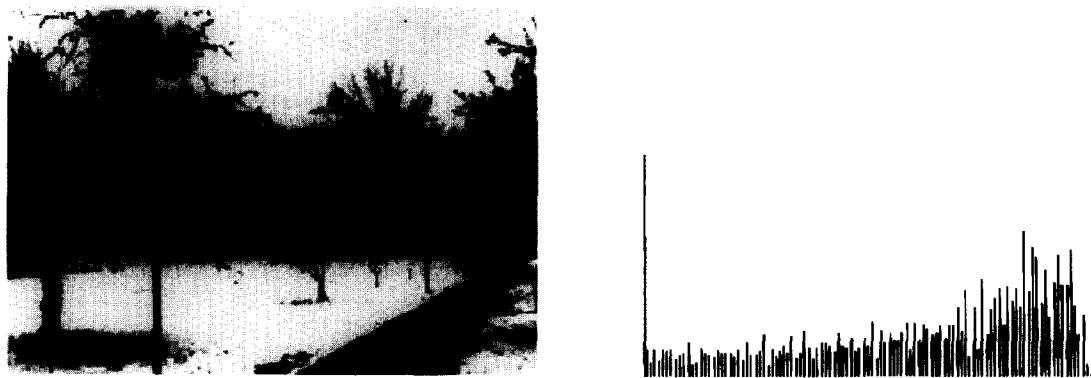


Fig. 25. Original digitized image of UofL campus and its histogram.

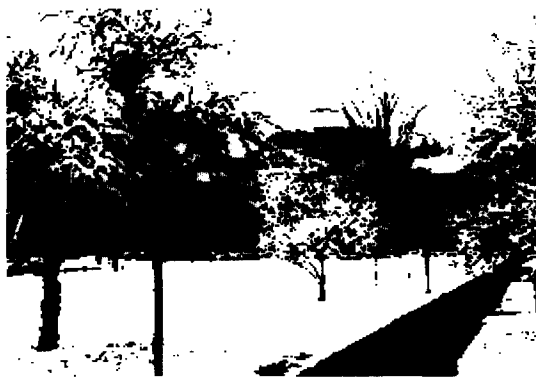


Fig. 26. Thresholded at $t_c^* = 155$.

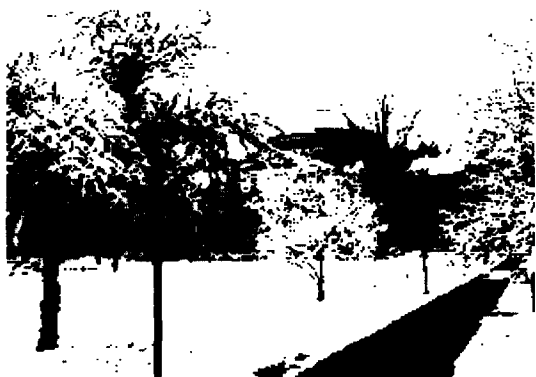


Fig. 27. Thresholded at $t_c^* = 177$.



Fig. 28. Thresholded at $t_2^* = 99$.

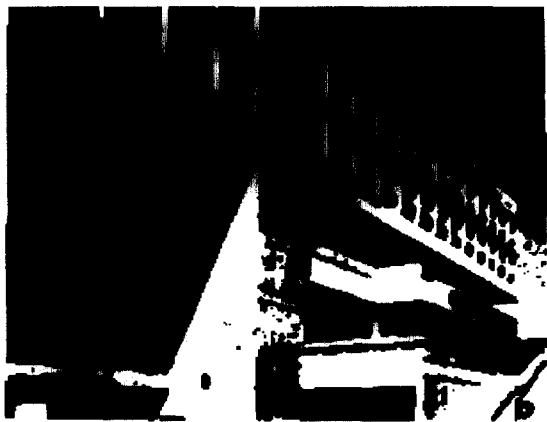


Fig. 29. Thresholded at $t_3^* = 145$.

We examined many images where both the entropic correlation method and the maximum entropy sum method failed to produce good threshold values. However when we apply the new method, we always find a very good threshold value. Recall that the optimal threshold value t_c^* was computed by the

formula

$$t_c^* = t_{[1]} \left[p(t_{[1]}) + \frac{1}{4} \omega \beta_1 \right] + \frac{1}{4} t_{[2]} \omega \beta_2 + t_{[3]} \left[1 - p(t_{[3]}) + \frac{1}{4} \omega \beta_3 \right],$$



Fig. 30. Thresholded at $t_2^* = 41$.

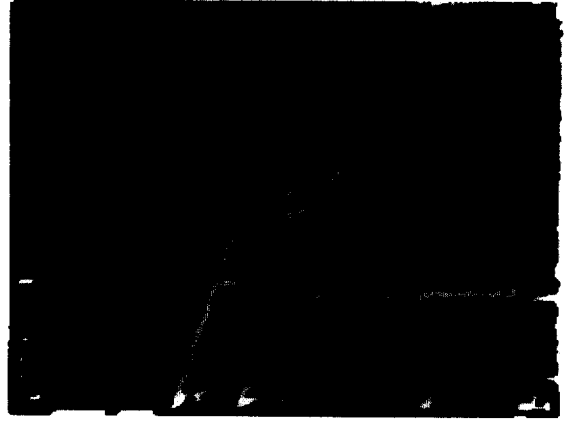


Fig. 31. Thresholded at $t_3^* = 18$.



Fig. 32. Thresholded at $t_2^* = 114$.



Fig. 33. Thresholded at $t_3^* = 139$.



Fig. 34. Thresholded at $t_2^* = 120$.



Fig. 35. Thresholded at $t_3^* = 168$.



Fig. 36. Thresholded at $t_2^* = 176$.



Fig. 37. Thresholded at $t_2^* = 132$.



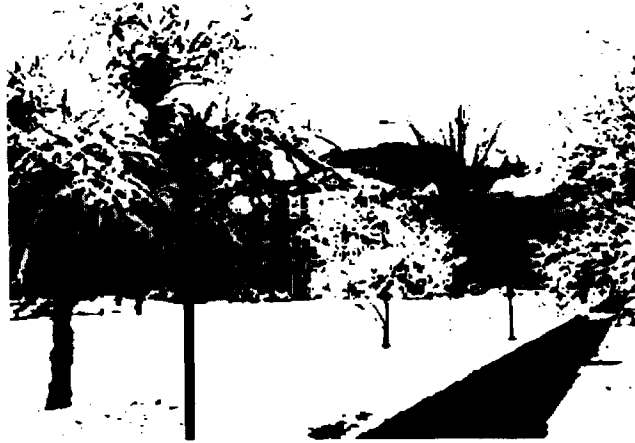
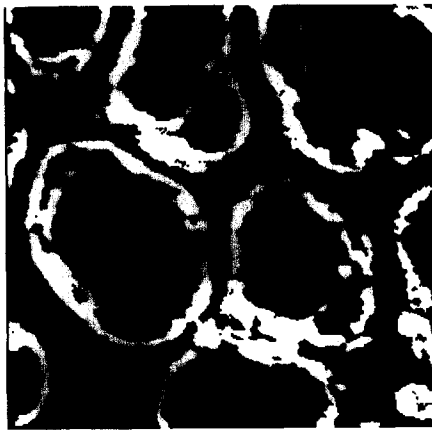
Fig. 38. Thresholded at $t_2^* = 119$.



Fig. 39. Thresholded at $t_2^* = 134$.

which can be rewritten as $t_c^* = w_1 t_{[1]} + w_2 t_{[2]} + w_3 t_{[3]}$, where w_1 , w_2 and w_3 are the weights determined by using local information. The new method incorporates global information obtained from the

gray-level histogram as well as local information embedded in the weights. Thus, it is not surprising that the proposed method yielded better threshold values.

Fig. 40. Thresholded at $t_2^* = 154$.Fig. 41. Thresholded at $t_2^* = 171$.

6. CONCLUSIONS

In this paper, we have developed a method that employs Renyi's entropy of order α to choose an optimal threshold value. This method of thresholding includes the maximum entropy sum method, and the entropic correlation method. In almost every image used, the proposed method yielded a better threshold value than that found by applying the maximum entropy sum method or the entropic correlation method. To our surprise we found that for a particular image $t^*(\alpha)$ is the same for every α between 0 and 1. Similarly, $t^*(\alpha)$ is the same (but different from the previous case) for every α between 1 and ∞ . We do not have a mathematical proof in this paper, as this result will be investigated elsewhere. A two-dimensional extension of this method can be developed similar to the method found by Abutaleb⁽⁷⁾ and Brink.⁽¹⁰⁾ This also will be treated in a forthcoming paper. Our bilevel method of thresholding can also be extended to multilevel thresholding with some appropriate modifications.

REFERENCES

1. B. Bhanu, Automatic target recognition: State of the art survey, *IEEE AES-22*, 364–379 (1986).
2. P. Yeh, S. Antoy, A. Litcher and A. Rosenfeld, Address location on envelopes, Center for Automation Research, University of Maryland, 213–227 (1986).
3. P. K. Sahoo, S. Soltani, A. K. C. Wong and Y. C. Chen A survey of the thresholding techniques, *Computing Vision Graphics Image Process.* **41**, 233–260 (1988).
4. J. S. Weszka, A survey of threshold selection techniques, *Computing Vision Graphics Image Process.* **7**, 259–265 (1978).
5. J. N. Kapur, P. K. Sahoo and A. K. C. Wong, A new method for gray level picture thresholding using the entropy of the histogram, *Computing Vision Graphics Image Process.* **29**, 273–285 (1985).
6. F. J. Chang, J. C. Yen and S. Chang, A new criterion for automatic multilevel thresholding, *IEEE Trans. Image Process.* **4**, 370–378 (1995).
7. A. S. Abutaleb, Automatic thresholding of grey-level pictures using two-dimensional entropies, *Pattern Recognition* **47**, 22–32 (1989).
8. N. Ahuja and A. Rosenfeld, A note on the use of second-order gray-level statistics for threshold selection, *IEEE Trans. Systems Man Cybernet.* **SMC-8**, 895–898 (1978).
9. B. Bhanu and O. D. Faugeras, Segmentation of images having unimodal distribution, *IEEE Trans. Pattern Analysis Mach. Intell.* **PCMI-4**, 408–419 (1982).
10. A. D. Brink, Thresholding of digital images using two-dimensional entropies, *Pattern Recognition* **25**, 803–808 (1992).
11. C. Chang, K. Chen, J. Wang and M. L. G. Althouse, A relative entropy based approach to image thresholding, *Pattern Recognition* **27**, 1275–1289 (1994).
12. S. C. Cheng and W. H. Tsai, A neural network implementation of the moment-preserving technique and its application to thresholding, *IEEE Trans. Comput.* **42**, 501–507 (1993).
13. L. Cinque, S. Levialdi and A. Rosenfeld, Fast pyramidal algorithms for image thresholding, *Pattern Recognition* **28**, 901–906 (1995).
14. L. S. Davis, A. Rosenfeld and J. S. Weszka, Region extraction by averaging and thresholding, *IEEE Trans. Systems Man Cybernet.* **SMC-5**, 383–388 (1975).
15. S. M. Fernando and D. M. Monro, Variable thresholding applied to angiography, *Proc. 6th Int. Conf. Pattern Recognition*, 152–156 (1982) (1975).
16. B. Forte and P. K. Sahoo, Minimal loss of information and optimal thresholding for digital images, Center for Information Theory, Waterloo, Ontario, Canada (1986).

17. K. S. Fu and J. K. Mui, A survey on image segmentation, *Pattern Recognition* **13**, 3–16 (1980).
18. L. Halada and G. A. Ososkov, Histogram concavity analysis by quasicurvature, *Comput. Artificial Intell.* **6**, 523–533 (1987).
19. L. Hertz and R. W. Schafer, Multilevel thresholding using edge matching, *Computing Vision Graphics Image Process.* **44**, 279–295 (1988).
20. L. Huang and M. J. Wang, Image thresholding by minimizing the measures of fuzziness, *Pattern Recognition* **28**, 41–51 (1995).
21. G. Johannsen and J. Bille, A threshold selection method using information measures, *6th Int. Conf. Pattern Recognition*, Munich, Germany (1982).
22. M. Kamel and A. Zhao, Extraction of binary character graphics images from gray scale document images, *CVGIP: Graphic Models and Image Process.* **55**, 203–217 (1993).
23. R. L. Kirby and A. Rosenfeld, A note on the use of (Gray level, Local average gray level) space as an aid in threshold selection, *IEEE Trans. Systems Man Cybernet.* **SMC-9**, 860–864 (1979).
24. T. Kurita, N. Otsu and N. Abdelmalek, Maximum likelihood thresholding based on population mixture models, *Pattern Recognition* **25**, 1231–1240 (1992).
25. S. U. Lee and S. Y. Chung, A comparative performance study of several global thresholding techniques for segmentation, *Computing Vision Graphics Image Process.* **52**, 171–190 (1990).
26. C. H. Li and C. K. Lee, Minimum cross entropy thresholding, *Pattern Recognition* **26**, 617–625 (1993).
27. P. K. Lim, M. A. Sid-Ahmed and G. A. Jullien, VLSI implementation of a digital image threshold selection architecture, *Integration, J. VLSI* **7**, 77–91 (1989).
28. F. Morii, An image thresholding method using a minimum weighted squared-distortion criterion, *Pattern Recognition* **28**, 1063–1071 (1995).
29. F. Morii, A note on minimum error thresholding, *Pattern Recognition Lett.* **12**, 349–351 (1991).
30. J. Olivo, Automatic threshold selection using the wavelet transform, *CVGIP: Graphical Models Image Process.* **56**, 205–218 (1994).
31. N. Otsu, A threshold selection method from gray-level histogram, *IEEE Trans. Systems Man Cybernet.* **SMC-8**, 62–66 (1978).
32. N. R. Pal and S. K. Pal, Entropic thresholding, *Signal Process.* **16**, 97–108 (1989).
33. N. Papamarkos and B. Gatos, A new approach for multilevel threshold selection, *CVGIP: Graphical Models Image Process.* **56**, 357–370 (1994).
34. J. G. Postaire and M. Ameziane, A pattern classification approach to multilevel thresholding for image segmentation, *Computer Vision and Image Processing*, L. Sapiro and A. Rosenfeld, eds, pp. 307–328 (1992).
35. T. Pun, Entropic thresholding, a new method, *Comput. Graphics Image Process.* **CGIP 16**, 210–239 (1981).
36. T. W. Ridler and S. Calvard, Picture thresholding using iterating selection method, *IEEE Trans. Systems Man Cybernet.* **SMC-8**, 630–632 (1978).
37. A. Rosenfeld and R. C. Smith, Thresholding using relaxation, *IEEE Trans. Pattern Analysis Mach. Intell.* **PAMI-3**, 598–606 (1981).
38. S. C. Sahasrabudhe and K. S. Das Gupta, A valley-seeking threshold selection technique, in *Computer Vision and Image Processing*, L. Sapiro and A. Rosenfeld, eds, pp. 55–65. (1992).
39. P. K. Sahoo, A. A. Farag and Y. P. Yeap, Threshold selection based on histogram modeling, *Proc. 1992 IEEE Conf. Systems Man and Cybernetics*, Chicago, 351–356 (1992).
40. A. G. Shanbhag, Utilization of information measure as a means of image thresholding, *CVGIP: Graphical Models Image Process.* **56**, 414–419 (1994).
41. H. J. Trussell, Comments on picture thresholding using an iterative selection method, *IEEE Trans. Systems Man Cybernet.* **SMC 9**, 311 (1979).
42. J. S. Weszka, R. N. Nagel and A. Rosenfeld, A threshold selection technique, *IEEE Trans. Comput.* **C-23**, 1322–1326 (1974).
43. J. S. Weszka and A. Rosenfeld, Histogram modification for threshold selection, *IEEE Trans. Systems Man Cybernet.* **SMC-9**, 38–52 (1979).
44. R. J. Whatmouth, Automatic threshold selection from a histogram using the exponential hull, *Computing Vision Graphics Image Process.* **53**, 592–600 (1991).
45. A. K. C. Wong and P. K. Sahoo, A gray-level thresholding selection method based on maximum entropy principle, *IEEE Trans. Systems Man Cybernet.* **19**, 866–871 (1989).
46. A. Y. Wu, T. Hong and A. Rosenfeld, Threshold selection using quad-tree, *IEEE Trans. Pattern Analysis Mach. Intell.* **PAMI-4**, 90–93 (1982).
47. A. Beghdadi and N. égrate, A. L.P. V. De Lesegno, Entropic thresholding using a block source model, *Graphical Models Image Process.* **57**, 197–205 (1995).
48. A. Renyi, On measures of entropy and information, *Proc. Fourth Berkeley Symp. Math. Statist. Prob.* **1960 1**, pp. 547–561. University of California Press, Berkeley (1961).

About the Author—PRASANNA SAHOO received his Ph.D. degree in Applied Mathematics from the University of Waterloo, Canada in 1986. He joined the staff of the University of Louisville in 1988, where he is an Associate Professor of Mathematics. He has authored more than 60 archival journal papers in areas such as functional equations, geometry, cryptography, mathematical economics and digital image processing.

About the Author—CARRYE WILKINS is a mathematics instructor at the University of Louisville, where she received her M.A. degree in Mathematics in 1994. Her research interest is in computer vision and its applications.

About the Author—JERRY YEAGER received his M.A. degree in Mathematics in 1991. He is currently a doctoral candidate in Urban and Public Affairs at the University of Louisville.